Research article **Journal of Human, Health and Halal Metrics; 2020, 1(1): 42-56**
https://doi.org/10.30502/JHHHM.2020.107920

Study of Reactive Red 195 anionic dye adsorption on calcined marble powder as potential eco-friendly adsorbent

Samaneh Farrokhzadeh[1*], Habib Razmi[1], Behrooz Jannat[2]

1- Analytical Chemistry Research Lab, Faculty of Basic Sciences, Azarbaijan Shahid Madani University, Tabriz, Iran.
2- Halal Research Center of IRI, FDA, Tehran, Iran.

Submission: 24 February 2020 ***Revision***: 26 February 2020 ***Acceptance***: 10 March 2020

Abstract

Background and objective: Recently, use of inexpensive and available adsorbents have been studied for removal purposes. One of main sources of environmental pollutions is uncontrolled discharge of wastewater containing synthetic dyes that may result in adverse effect on human health. At this study, removal efficiency of marble powder (MP) and calcined marble powder (CMP) as potential and low cost natural adsorbents for removal of Reactive Red 195 as anionic dye was investigated.

Materials and methods: The adsorbents were characterized by X-Ray diffraction, Fourier Transform Infrared spectroscopy, scanning electron microscopy and zeta potential measurements. Anionic dye of Reactive Red 195 was used as adsorbate. Raw MP was collected from marble processing plant and its calcination was done at 750°C for 3 h in furnace.

Results and conclusion: Effect of variables including pH, adsorbent dose, contact time, dye concentration and temperature were monitored by a batch system. Adsorption reactions at equilibrium followed Langmuir isotherm and pseudo-second order kinetic models. Maximum adsorption capacity of 103.092 mg g^{-1} was observed for CMP that was more than MP (1.218 mg g^{-1}). Results showed that calcination process can significantly reduce negative charges on surface of marble powder and promote its efficiency for anionic dye removal. Thermodynamic study revealed that adsorption of Reactive Red 195 on CMP was exothermic and spontaneously. In conclusion, abundance of MP as inorganic waste and its transformation to CMP by simple calcination process makes it an efficient, available and economic candidate for water purification.

Keywords: Adsorption isotherm, calcined marble powder, kinetic, Reactive Red 195, removal

1. Introduction

Nowadays, one of important sources of environmental pollution is chemical coloring agents in wastewater such as those released from textile factories [1]. Approximately, more than 10000 dyes of different origin are produced and consumed commercially, of which nearly 30% are not stable and make toxicity to the environment. Reactive dyes have interfering effects on aquatic ecosystems even at low

[*] Correspondence to: Samaneh Farrokhzadeh; e-mail: Samanehfarrokhzadeh@azaruniv.ac.ir; Tel.: +98-4134327500; Fax: +98-4134327541

quantities by inhibition of sunlight penetration into water and impair photosynthesis [2–6]. In addition, they have carcinogenic effect on living cells. Reactive azo dyes are popular because of their low cost, variety, good solubility and stability in water [7,8]. Due to high stability and complex chemical structure, they are resistant against physical, chemical and biological treatments [9]. Therefore, there is a concern on their removal from environment and further possible health issues threating the habitants. In this regard, some treatments based on physical, chemical and biological processes are used such as membrane filtration, coagulation, microbial biodegradation, oxidation, ozonation and bio-sorption [1,10–12]. However, there is great attention to develop alternative techniques due to some practical or economical restrictions [13]. Among them, adsorption process is advantageous due to its simplicity, high efficiency and applicability for various pollutants [11,14,15]. Recently, use of inexpensive and available adsorbents containing clay-derived chemicals such as bentonite, perlite, lignite, silica, zeolite, peat, Kaolin and agricultural/industrial waste have been studied [16–22]. Marble powder (MP) is inorganic adsorbent, which is frequently found in Spain, Eygept, Greece, Turkey and Iran. It contains chemical ingredients of $CaCO_3$, SiO_2, Al_2O_3, MgO, Fe_2O_3, K_2O and Na_2O. MB is produced through building and manufacturing operations and has been used as available, abundant and low-cost inorganic adsorbent for treatment of dye contaminated waters [23,24]. For example, desirable results were observed for its efficiency in methylene blue removal [24]. Interestingly, calcination process can significantly increase its ability. Therefore, transformation of MB to calcined form by simple process introduced it an efficient, economic, available and high potential candidate for this purpose. At this study, adsorption characteristics of raw MB and calcined marble powder (CMP) was examined to find out an applicable way in protection of environment, animals, plants and human against deteriorative agents. Reactive Red 195, a toxic anionic azo dye with five sulfonic groups (Figure 1), was selected as model. Effect of pH, adsorbent dose, contact time, dye concentration and temperature on adsorption were studied. At the end, isotherm, kinetic and thermodynamic behaviors of process are discussed.

2. Materials and methods

2.1. Materials

Anionic dye of Reactive Red 195 was supplied by Merck (Darmstadt, Germany). The chemical structure of dye was given in Figure 1.

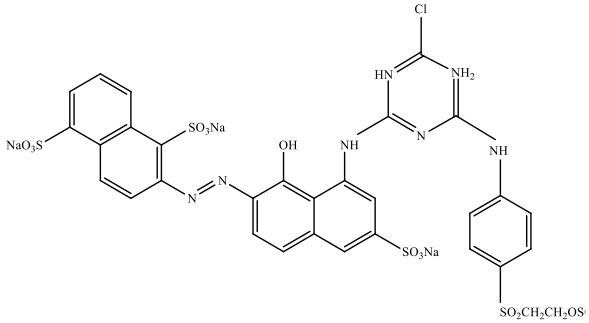

Figure 1- Chemical structure of Reactive Red 195

Stock solution of Reactive Red 195 at concentration of 1000 mg l^{-1} was prepared and further dilutions were made by addition of double distilled water. Sodium hydroxide and hydrochloric acid were purchased from Merck (Darmstadt, Germany) and concentration of 0.1 mol l^{-1} was used for pH adjustment. Absorbance of solutions was measured at λ_{max}=517 nm before and after reactions. MP was collected from a marble processing factory located in Tehran (Iran).

2.2. Preparation of calcined marble powder

Raw MP was washed several times by distilled water and dried at 60°C for 12 h. Dried sample was sieved to get particles of 75 μm. Then, raw powder was calcined at 750°C for 3 h in furnace [25,26]. CMP was stored in a falcon tubes for further experiments.

2.3. Apparatus

X-ray diffraction (XRD) analysis were carried out using Bruker AXF (D8 Advance) diffractometer with Cu K_α radiation in 2θ angle ranging from 10º to 80º. Fourier transform infrared (FT-IR) Spectrometer (Bruker model Vector 22, Ettlingen, Germany) in range 500-4000 wavenumber (cm^{-1}) was used. Scanning electron microscopy (SEM) imaging for observation of surface morphology was done by S-4800 Hitachi scanning electron microscope (Japan). Centrifugation at 958 ×g for 15 min was done to separate adsorbent solid particles from supernatant. Absorption of supernatant was read at 517 nm by UV-VIS spectrophotometer model T80. Zeta potential of MP and CMP was measured using Malvern instrument (UK). pH of dye solution was measured using Metrohm 744 pH-meter.

2.4. Adsorption experiment

Adsorption process of Reactive Red 195 on MP and CMP was carried out through a batch system. A series of 25 ml of dye solution in various concentrations were prepared and poured into a beaker of 50 ml, separately, followed by addition of a known dose of MP and CMP. The mixture was stirred for 1 to 50 min at room temperature by magnetic stirrer. After achieving steady state adsorption in the experiment (approximately 30 min), 3 ml of mixture was drawn and centrifuged at 958 ×g for 15 min. Absorbance of residual dye in supernatant was read at λ_{max}=517 nm in UV-VIS spectrometer. Adsorption percent of Reactive Red 195 on the adsorbents (R%), and adsorbed amount of Reactive Red 195 per unit mass of the adsorbent at equilibrium (q_e: mg g^{-1}) are calculated by following equations (Eq. 1 and 2):

$$R(\%) = \frac{(C_0 - C_e)}{C_0} \times 100 \qquad \text{Eq. 1}$$

$$q_e = \frac{(C_0 - C_e)\,V}{m} \qquad \text{Eq. 2}$$

Where, C_o and C_e are dye concentration at time 0 and equilibrium (mg l^{-1}), respectively; V is volume of Reactive Red 195 solution (l) and m is MP and CMP mass (g). q_e (mg g^{-1}) is amount of adsorbed Reactive Red 195 per g of MP and CMP.

3. Results and discussion

3.1. Characterization of adsorbents

X-ray diffraction analysis was done to study the crystallinity of MP and CMP. XRD patterns provide convincing evidence about change of calcite phase of MP to CaO phase. As shown in Figure 2, main diffraction peak of MP is observed at 2θ=29.720˚ and other peaks at 2θ=23.360˚, 39.720˚ and 47.800˚ correspond to diffraction of calcite phase ($CaCO_3$) [24]. Furthermore, there are other peaks at 2θ=29.720˚and 65˚ for SiO_2, at 2θ=43.440˚ for $Mg(OH)_2$ and weak peaks for the other residual components [23,24]. In comparison to MP, intensity of $CaCO_3$ peak (main peak of calcite phase) was little in CMP showing that calcite phase was significantly transformed to CaO through calcination process (Figure 2). With regard, CaO phase peaks approximately at 2θ=32º, 37º, 54º, 64º and 67º were emerged for calcined powder.

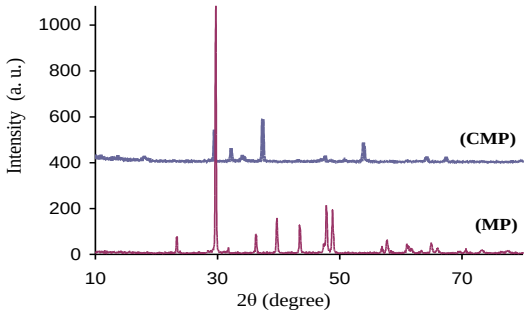

Figure 2- XRD patterns of MP and CMP

FT-IR spectra of MP and CMP are presented in Figure 3. Spectrum of MP clearly shows the bands of calcite phase ($CaCO_3$) at 712, 1418, 1800 and 2515 cm^{-1} [24]. Weak peaks at 1800 cm^{-1} and 2515 cm^{-1} refer to C=O group and HCO_3^- in calcite structure [23]. In comparison, FT-IR spectrum of CMP shows that intensity of calcite phase decreased and a new peak at 3643 cm^{-1} emerged owing to stretching OH in $Ca(OH)_2$ that formed by water adsorption on CaO component [27].

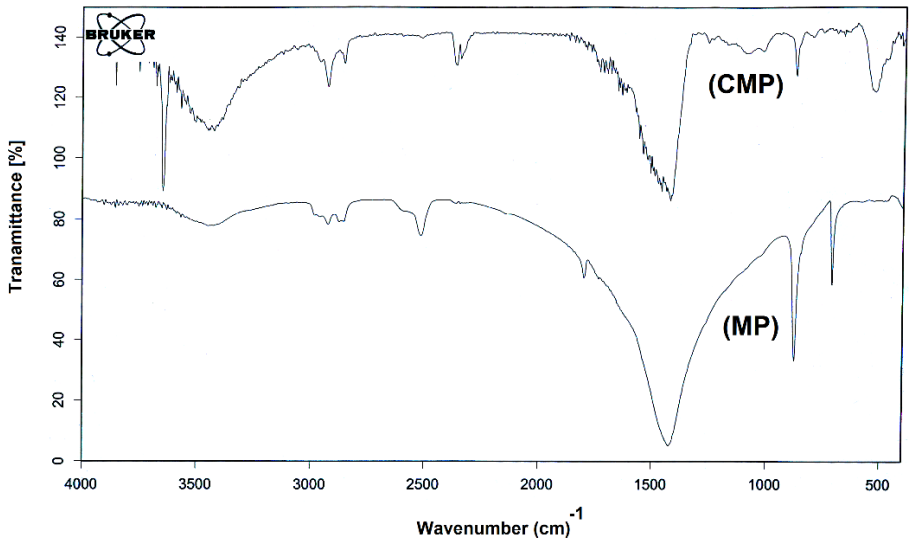

Figure 3- Fourier transform infrared spectra of MP and CMP

SEM images and surface morphology of MP and CMP are shown in Figure 4. As can be seen, MP shows a rigid structure (Figure 4A) while CMP has fine and soft surface (Figure 4B) that facilitates effective dye adsorption on its porous and homogenous structure.

Zeta potential describes electric charge distribution on material surface. It reflects electrostatic interactions between adsorbate and adsorbent and can evaluate stability of colloidal dispersion. Relevantly, high zeta potential in colloidal dispersions prevents particles' aggregation and prolonged stability of system is expected. Figure 5 shows zeta potential of MP and CMP under same condition (pH=9, T=25°C). As can be seen in the figure, zeta potential of −20.060 mV was detected for MP and positive zeta potential of +22.040 mV was detected for CMP. Based on the results, repulsive electrostatic forces between MP and anionic dye caused poor adsorption efficiency compared to attractive electrostatic forces between CMP and anionic that resulted in better adsorption.

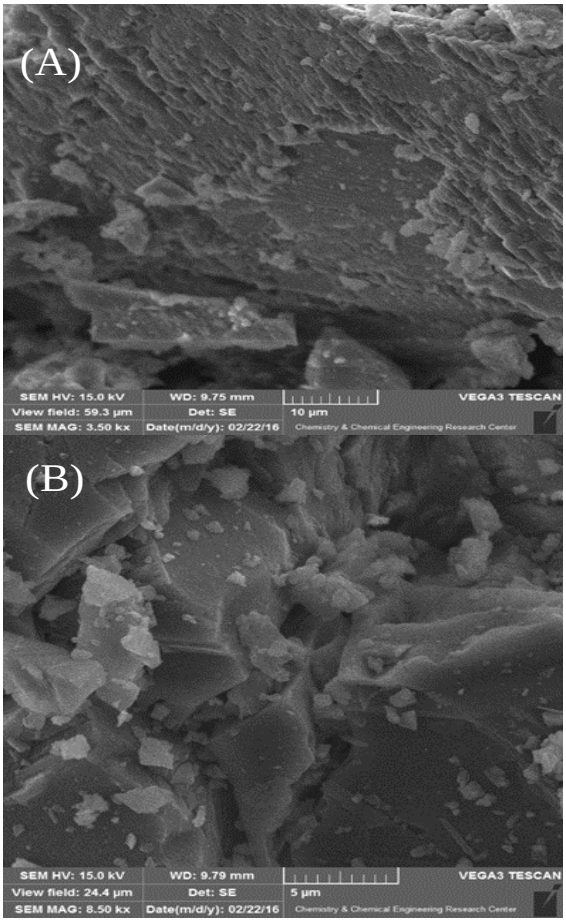

Figure 4- SEM images of A) MP and B) CMP

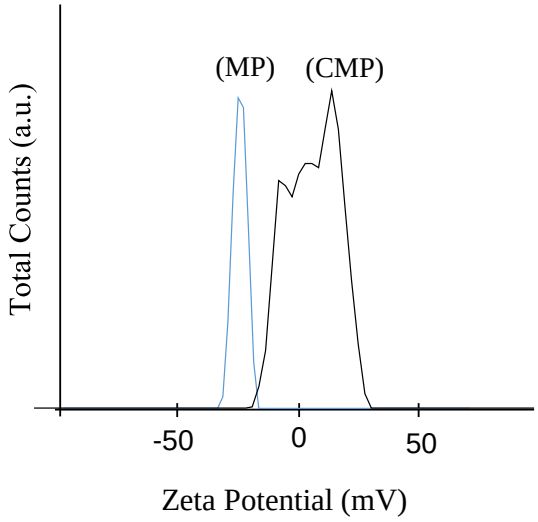

Figure 5- Zeta potential analysis of MP and CMP

3.2. Influence of effective variables on adsorption process

Experimental design provides some advantages such as finding optimum condition of trials. In our study, one-factor-at-a-time (OFAT) approach was used to find out optimum levels of main effective variables for further experiments.

3.2.1. Effect of pH on adsorption capacity

Due to the fact that pH of solution largely influences electrostatic interactions, this variable was examined. Therefore, a couple of dye solution were prepared at various pH ranging from 2 to 12. To find optimum point, dye adsorption on CMP was measured and its efficiency remained constant in all cases. pH of dye solutions was measured after addition of certain dose of CMP. All samples showed alkaline pH (10-12) despite different initial pH of dye solutions. Indeed, adjusted pH of dye solutions was rapidly changed upon addition of CMP (CaO-based adsorbent) to dye solution. This might be due to partial dissolution of alkaline metal oxides in CMP when it was exposed to dye solution during contact time. Therefore, one of the most advantages of CMP was its pH-independent efficiency.

3.2.2. Effect of adsorbent dose

Figure 6a shows impact of MP and CMP dose on the result. For both adsorbents, adsorption efficiency increased by increasing the adsorbent mass due to enhanced availability of active sites on the structure. Maximum dye removal efficiency was achieved by 2400 and 50 mg of MP and CMP, respectively. Adsorption level was not considerably changed at higher concentrations due to fully engagement of anionic dye (at constant concentration) on adsorbents' active sites. The results clearly confirmed that calcination could improve adsorption potential of CMP.

3.2.3. Effect of contact time

Contact time of dye solution with MP and CMP can control adsorption dynamics. To examine, some trials were conducted in range of 5 to 60 min at optimum adsorbent dose (50 and 2500 mg for CMP and MP) and dye concentration (100 mg l^{-1}) (Figure 6b). At first, amount of adsorbed dye per unit mass of CMP increased rapidly and then was constant until the end of study. The quick initial rise was probably due to abundance of free active sites on surface of the adsorbent that were available to dye interaction and then fully occupied at equilibrium. Therefore, optimum contact time for Reactive Red 195 removal by MP and CMP was 30 and 20 min, respectively.

3.2.4. Effect of initial dye concentration

Various initial dye concentrations ranging from 20 to 160 mg l^{-1} was studies at optimum adsorbent dose (50 and 2500 mg for CMP and MP, respectively) and contact time (20 and 30 min for CMP and MP, respectively). According to Figure 6c, adsorption increased by increasing the dye concentration. It may be related to abundance of active sites on adsorbents, enhanced driving force and decreased diffusion resistant for uptake of dye ions. Moreover, effective collisions of adsorbent and dye will increase at high concentrations [26, 28-32]. As a result, dye concentration up to 150 mg l^{-1} was introduced in practice.

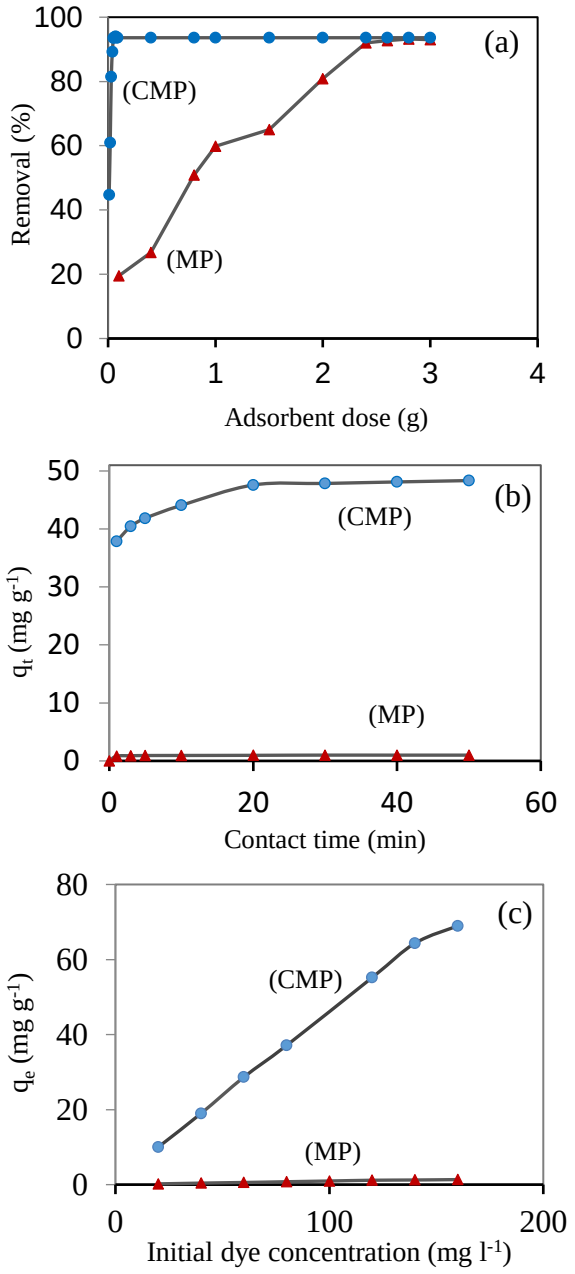

Figure 6- Effect of a) adsorbent dose, b) contact time and c) initial dye concentration on Reactive Red 195 adsorption by MP and CMP

3.2.5. Effect of temperature

This study was carried out in range of 30–70°C. According to Figure 7, adsorption capacity of CMP was decreased at high temperature [33, 34]. In comparison, the changes were not significant for MP might be due to its lower adsorption capacity.

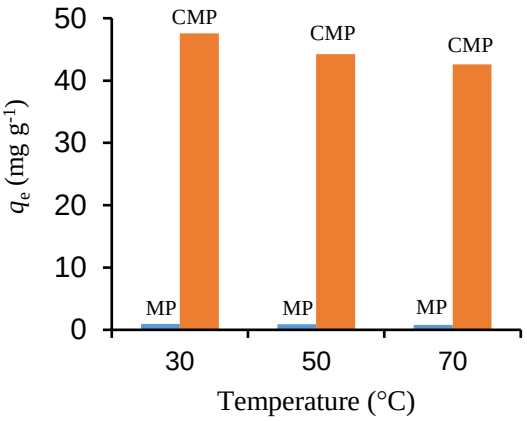

Figure 7- Effect of temperature on adsorption of Reactive Red 195 on MP and CMP

3.3. Adsorption isotherms

Adsorption isotherms show distribution equilibrium of adsorbate between aquatic solution and adsorbent. Adsorption equilibrium data were obtained by using different initial dye concentrations at constant time. Then, data were analysed by isotherm models of Langmuir, Freundlich, Tempkin and Dubinin-Radushkevich (D-R) through which the best model that appropriately fitted to the adsorbate/adsorbent interaction was selected. Langmuir isotherm linear equation (Eq. 3) that corresponds to monolayer sorption of adsorbate molecules on homogenous surface of adsorbent [32] is expressed as follows:

$$\frac{1}{q_e} = \frac{1}{(k_L\, q_m c_e)} + \frac{1}{q_m} \qquad \text{Eq. 3}$$

Where, q_e is amount of adsorbed dye at equilibrium (mg g^{-1}), C_e is equilibrium concentration of dye solution (mg l^{-1}), q_m is maximum adsorption capacity of adsorbent (mg g^{-1}), k_L is Langmuir constant corresponding to free energy of adsorption process (l mg^{-1}) (Figure 8A). Equilibrium parameter, R_L, is an important factor for shape prediction of isotherm and describes favorability ($0<R_L<1$), linearity ($R_L=1$), irreversibility ($R_L=0$), and unfavorability ($R_L>1$). Adsorption features of Langmuir isotherm is expressed by following equation [21]:

$$R_L = \frac{1}{1+ k_L c_o} \quad \text{Eq. 4}$$

All values of R_L in present study were between 0 and 1 (Table 1 and Figure 8B) indicating that MP and CMP were favorable inorganic adsorbents of Reactive Red 195 under optimized experimental condition.

In contrast, Freundlich isotherm is based on multilayer adsorption with a uniform distribution of sorption heat over heterogeneous surface. Linearized form of Freundlich isotherm is:

$$\ln q_e = \ln k_F + \left(\frac{1}{n}\right) \ln c_e \quad \text{Eq. 5}$$

Where, k_F is Freundlich constant ($mg^{1-(1/n)}\ g^{-1}\ L^{1/n}$) and n is extent of deviation from linearity of process that used to determine linear (n=1), physical (n>1) and (n<1) chemical type of reaction. At this study, n=2.32 and n=1.83 was calculated for dye adsorption on MP and CMP which confirmed that the dye was physically adsorbed.

Tempkin isotherm studies heat transfer between adsorbate and adsorbent [35]. Its linearized equation is expressed as follows:

$$q_e = B \ln A + B \ln C_e \quad \text{Eq. 6}$$

Where, B is constant and related to heat of sorption process. It is calculated from B=RT/b equation; i.e., b is constant of Tempkin isotherm (J mol^{-1}), R is gas constant (8.314 $Jmol^{-1}K$), T is absolute temperature (°K) and A is equilibrium binding constant (l mg^{-1}).

To provide energetic information about mechanism and type of dye adsorption on adsorbent, D-R isotherm was studied [31,36]. The linear form of D-R isotherm is shown in Eq. 7.

$$\text{Ln } q_e = \ln q_m - K_{DR} \varepsilon^2 \quad \text{Eq. 7}$$

Where, q_e is adsorbed amount of dye per unit mass of adsorbent (mg g^{-1}), q_m is adsorption capacity related to D-R isotherm (mg g^{-1}), K_{DR} is a constant related to adsorption energy ($mol^2\ J^{-2}$) and ε is Polanyi potential given by equation 8.

$$\varepsilon = RT \ln\left(1 + \frac{1}{C_e}\right) \quad \text{Eq. 8}$$

Parameter of E (declared in Eq. 9) is used to determine nature of adsorption process. This parameter is defined as mean free energy of process in transfer of one mole adsorbate on adsorbent surface and its magnitude is calculated according to following equation [36,37].

$$E = \frac{1}{\sqrt{2K_{DR}}} \quad \text{Eq. 9}$$

Magnitude of E predicts whether adsorption is conducted by physical (E<8 kJ mol^{-1}), ion exchange (8<E<16 kJ mol^{-1}) or chemical (E>16 kJ mol^{-1}) interactions [38]. In our study, E values were 1.580 and 0.700 kJ mol^{-1} for MP and CMP suggesting that the adsorption process was physical in nature.

Plots of isotherms for Reactive Red 195 adsorption on MP and CMP are shown in Figure 8a-e and isotherm parameters are summarized at Table 1.

Correlation coefficients (R^2) of isotherm equations state that the equilibrium adsorption data are well explained by Langmuir isotherm model. Based on this finding, monolayer adsorption of dye on MP and CMP was occurred.

It is important to analyze errors of experimental and calculated values to evaluate fitness of empirical equilibrium data. At this work, a non-linear Chi-Square test was used [39] that is according to the following mathematical equation:

$$X^2 = \sum_{i=m}^{1} \frac{\left(q_{e,\,\exp} - q_{e,\,\text{cal}}\right)^2}{q_{e,\,\exp}} \quad \text{Eq. 10}$$

Where, $q_{e,exp}$ and $q_{e,cal}$ are equilibrium capacity obtained from experiment and calculation (mg g^{-1}), respectively. If $q_{e,exp}$ is similar to $q_{e,cal}$, it will be the best fitted isotherm for adsorption system. According to the calculated values of X^2 for isotherm models in our study, Langmuir isotherm model was the best.

3.4. Adsorption Kinetics

Kinetic of adsorption process depends on physical and chemical properties of adsorbent and transfer of adsorbate mass on adsorbent surface [40,41]. Dynamic of Reactive Red 195 adsorption on MP and CMP was investigated by various models including pseudo-first order, pseudo-second order, intra-particle diffusion and Elovich [42,43]. The linearized equation of pseudo-first order kinetic is shown in Eq.11 [42].

$$\log (q_e - q_t) = \log (q_e) - \frac{k_1 t}{2.303} \qquad \text{Eq. 11}$$

In the equation, q_e and q_t (mg g^{-1}) are adsorption capacity at equilibrium and any time, respectively, and k_1 is rate constant of first order kinetic model (min^{-1}). In pseudo-second order kinetic model, rate-limiting step is chemisorption [44]. This model is expressed as follows:

$$\frac{t}{q_t} = \frac{1}{k_2 q_e^2} + \frac{t}{q_e} \qquad \text{Eq. 12}$$

In the equation, k_2 is rate constant of pseudo-second order equation (g mg^{-1} min^{-1}).

Intra-particle diffusion model (Weber-Morris model) elucidates mechanism of dye absorption into pores of adsorbent [45]. Equation of intra-particle diffusion was proposed by Weber-Morris model (Eq. 13):

$$q_t = k_{dif}\, t^{0.5} + C \qquad \text{Eq. 13}$$

Where, k_{dif} is rate constant of intra-particle diffusion model (mg g^{-1} $min^{-0.5}$), and C is thickness of boundary layer (mg g^{-1}).

Elovich kinetic model describes heterogeneous adsorption energy over the adsorbent surface (Weber and Morris). The kinetic equation for this model was expressed in Eq. 14:

$$q_t = \frac{1}{\beta} \ln (\alpha\beta) + \frac{1}{\beta} \ln (t) \qquad \text{Eq. 14}$$

Where, α (mg g^{-1} min^{-1}) and β (g mg^{-1}) are rate constants for Elovich equation and represent the magnitude of surface coverage.

The kinetic curves are depicted in Figure 9a-d and the fitness parameters are shown at Table 2.

According to Table 2, value of q_e calculated from pseudo-second order model was close to experimental q_e for both MP and CMP. Moreover, a linear response with high correlation coefficients for t/q_t against t indicated that the process could be described by pseudo-second order kinetic.

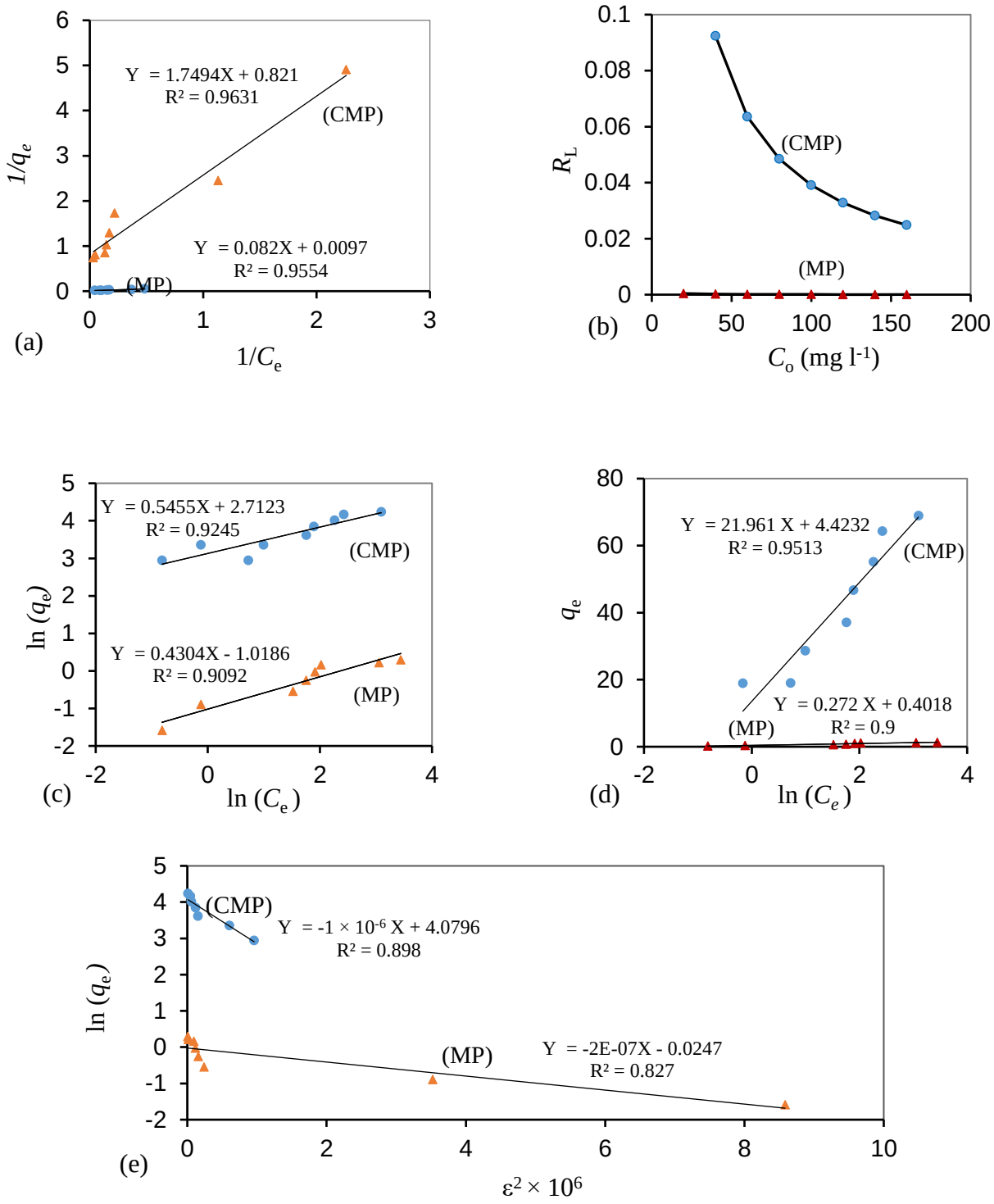

Figure 8- Plots of adsorption isotherms obtained for adsorption of Reactive Red 195 on MP and CMP: a) Langmuir, b) values of R_L, c) Freundlich, d) Tempkin and e) Dubinin-Radushkevich isotherm models.

Table 1- Isotherm parameters for adsorption of Reactive Red 195 on MP and CMP

Isotherm	Parameters	MP	CMP
Langmuir	q_m (mg g^{-1})	1.218	103.092
$1/q_e = 1/(k_a q_m c_e) + 1/q_m$	k_L (l mg^{-1})	0.469	0.118
	R_L	0.096-0.013	0.174-0.050
	χ^2	0.222	2.124
	R^2	0.963	0.955
Freundlich	n	2.323	1.830
$\ln q_e = \ln k_F + (1/n)\ln c_e$	k_F (l mg^{-1})	0.361	9.608
	R^2	0.909	0.924
	χ^2	0.206	4.850
Tempkin	B	0.272	21.961
$q_e = B\ln(A) + B\ln(C_e)$	A (l mg^{-1})	4.379	1.223
	R^2	0.900	0.951
	χ^2	0.162	2.128
D-R	q'_m(mg g^{-1})	0.975	59.120
$\ln q_e = \ln q'_m - k_{DR}\varepsilon^2$	K_{DR} (mol^2 J^{-2})	0.2 × 10^{-6}	1 × 10^{-6}
	E (kjmol^{-1})	1.581	0.707
	R^2	0.827	0.898

3.5. Adsorption thermodynamics

Impact of temperature on adsorption system of Reactive Red 195/MP and Reactive Red 195/CMP is evaluated by thermodynamic parameters to provide information about energy changes within the systems. Free energy (ΔG°, kJ mol^{-1}), enthalpy (ΔH°, kJ mol^{-1}) and entropy (ΔS°, J mol^{-1} K^{-1}) changes define thermodynamic nature of process. Magnitude of free energy (ΔG°) as important factor for spontaneity is determined by equations 15 and 16 [46-48].

$$\Delta G° = \Delta H° - T\Delta S° \quad \text{Eq. 15}$$

$$\Delta G° = -RT\ln k_c \quad \text{Eq. 16}$$

Where, R (8.314 J mol^{-1} K^{-1}) is gas constant, T (°K) is temperature and k_c (L mol^{-1}) is distribution coefficient that could be determined by the following equation (Eq. 17).

$$K_{(c)} = \frac{q_e}{C_e} \quad \text{Eq. 17}$$

Where, q_e is amount of dye adsorbed on adsorbent, and C_e is concentration of dye at equilibrium. ΔH° and ΔS° are calculated from slope and intercept of ln (k_c) against 1/T (Figure 10) according to equation 18.

$$\ln(k_c) = -\frac{\Delta H°}{RT} + \frac{\Delta S°}{R} \quad \text{Eq. 18}$$

Thermodynamic parameters are shown at Table 3. ΔG° for adsorption of dye on MP increased from 6.017 to 9.617 kJ mol^{-1} by increasing the temperature which shows non-spontaneity of adsorption process. In the case of CMP, the negative free energy confirmed that the process was spontaneous. Negative values of enthalpy change for both MP and CMP indicated an exothermic nature of adsorption and negative ΔS° showed a decreased randomness at solid–solute interface.

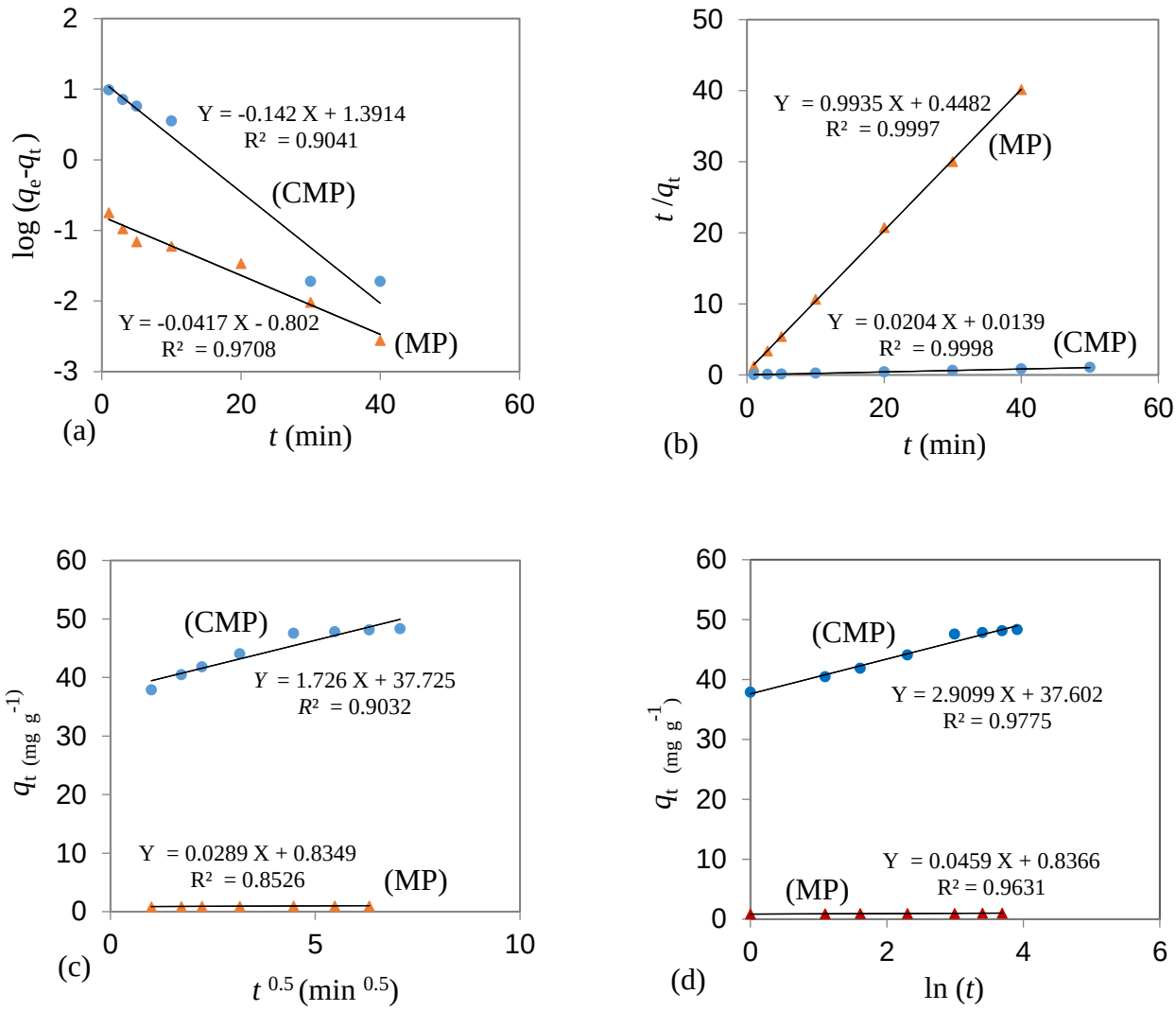

Figure 9- Kinetic models of Reactive Red 195 adsorption on MP and CMP: a) pseudo-first order, b) pseudo-second order, c) intra-particle diffusion and d) Elovich

Table 2- Kinetic parameters of Reactive Red 195 adsorption on MP and CMP

Model	Parameter	MP	CMP
Pseudo-first order	$q_{e,exp}$ (mg g^{-1})	0.999	47.580
$\log(q_e - q_t) = \log q_e - k_1 t / 2.303$	q_e (mg g^{-1})	0.448	1.391
	K_1 (min^{-1})	0.096	0.327
	R^2	0.970	0.904
Pseudo-second order	q_e (mg g^{-1})	1.006	49.010
$t/q_t = 1/k_2 q_e^{\ 2} + t/q_e$	K_2 (mg l^{-1} min^{-1})	2.202	0.029
	R^2	0.9997	0.9998
Intra-particle diffusion	C	0.834	37.725
$q_t = k_{dif} t^{0.5} + C$	K_{dif} (mg g^{-1} min$^{-0.5}$)	0.028	1.720
	R^2	0.852	0.903
Elovich	α (mg g^{-1} min^{-1})	37.8 × 10^5	11.9 × 10^5
$q_t = 1/\beta \ln(\alpha\beta) + 1/\beta \ln(t)$	β (g mg^{-1})	21.780	0.343
	R^2	0.963	0.977

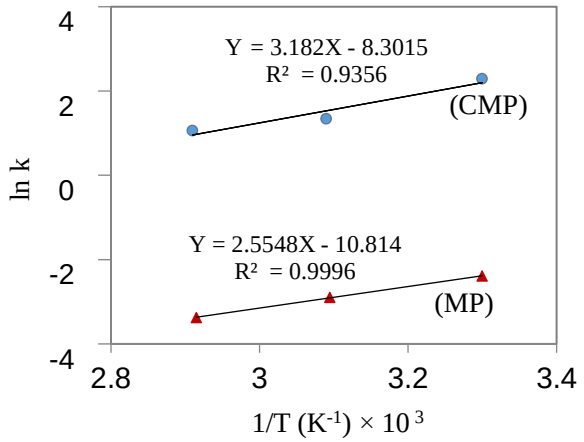

Figure 10- Effect of temperature on adsorption kinetic of Reactive Red 195 on MP and CMP

Table 3- Thermodynamic parameters of Reactive Red 195 adsorption on MP and CMP

Adsorbent	ΔG° (KJ mol^{-1})			ΔH° (J mol^{-1})	ΔS° (J mol^{-1} k^{-1})
	30°C	50°C	70°C		
MP	6.017	7.778	9.617	-21.090	-89.383
CMP	-5.758	-3.606	-3.021	-26.455	-69.018

4. Conclusion

CMP as a new, low-cost, available and high potential adsorbent was obtained by thermal treatment of MP. The calcination process could significantly enhance dye removal capacity of MP. The results revealed that Reactive Red 195 removal efficiency as an anionic pollutant was pH-independent. Experimental data were modeled by four adsorption isotherms through which Langmuir isotherm provided the best fitness to equilibrium data. Adsorption capacity of CMP for dye removal was significantly higher than MP that introduced it a potential candidate for wastewater treatment. Adsorption kinetic followed pseudo-second order model. Thermodynamic analysis revealed that removal of Reactive Red 195 from aqueous solution by CMP was spontaneous and through exothermic process.

5. Acknowledgement
The authors would like to appreciate the Research Council of Shahid Madani University for its financial assistance to the current work.

6. Conflict of interest
The authors have no conflict of interest.

References
1. Santhy K, Selvapathy P. Removal of reactive dyes from wastewater by adsorption on coir pith activated carbon. Bioresource Technology. 2006; 97: 1329–1336.
https://doi.org/10.1016/j.biortech.2005.05.016.

2. Aksu Z, Tezer S. Equilibrium and kinetic modelling of biosorption of Remazol Black B by Rhizopus arrhizus in a batch system: effect of temperature. Process Biochemistry. 2000; 36: 431-439.
https://doi.org/10.1016/S0032-9592(00)00233-8.

3. Robinson T, McMullan G, Marchant R, Nigam P. Remediation of dyes in textile effluent: a critical review on current treatment technologies with a proposed alternative. Bioresource Technology. 2001; 77: 247–255.
https://doi.org/10.1016/S0960-8524(00)00080-8.

4. Namasivayam C, Kavitha D. Removal of Congo Red from water by adsorption onto activated carbon prepared from coir pith, an agricultural solid waste. Dyes and Pigments. 2002; 54, 47–58.
https://doi.org/10.1016/S0143-7208(02)00025-6.

5. Iqbal MJ, Ashiq MN. Adsorption of dyes from aqueous solutions on activated charcoal. Journal of Hazardous Materials. 2007; 139: 57–66.
https://doi.org/10.1016/j.jhazmat.2006.06.007.

6. Samarghandi MR, Zarrabi M, sepehr MN, Amrane A, Safari GH, Bashiri S. Application of acidic treated pumice as an adsorbent for the removal of azo dye from aqueous solutions: kinetic, equilibrium and thermodynamic studies. Iranian Journal of Environmental Health Science and Engineering. 2012; 9: 1–10.
https://doi.org/10.1186/1735-2746-9-9.

7. Mittal A, ThakurV, Gajbe V. Evaluation of adsorption charac- teristics of an anionic azo dye Brilliant Yellow onto hen feathers in aqueous solutions. Environmental Science and Pollution Research. 2012; 19: 2438–2447.
https://doi.org/10.1007/s11356-012-0756-9.

8. Mittal A, Thakur V, Gajbe V. Adsorptive removal of toxic azo dye Amido Black 10B by hen feather. Environmental Science and Pollution Research. 2013; 20: 260–269.
https://doi.org/10.1007/s11356-012-0843-y.

9. Shokoohi R, Vatanpoor V, Zarrabi M, Vatani A. Adsorption of Acid Red 18 (AR18) by Activated Carbon from Poplar Wood- A Kinetic and Equilibrium Study. European Journal of Advanced Chemistry Research. 2010; 7(1): 65–72.
https://doi.org/10.1155/2010/958073.

10. McKay G, Porter JF, Prasad GR. The Removal of Dye Colours from Aqueous Solutions by Adsorption on Low-cost Materials. Water, Air and Soil Pollution. 1999; 114:423–438.
https://doi.org/10.1016/0043-1354(81)90036-1.

11. Baccar R, Bouzid J, Feki M, Montiel A. Preparation of activated carbon from Tunisian olive-waste cakes and its application for adsorption of heavy metal ions. Journla of Hazardous Materials. 2009; 162: 1522–1529.
https://doi.org/10.1016/j.jhazmat.2008.06.041.

12. Yang J, Qiu K. Preparation of activated carbons from walnut shells via vacuum chemical activation and their application for methylene blue removal. Chemical Engineering Journal. 2010; 165: 209–217.
https://doi.org/10.1016/j.cej.2010.09.019.

13. Aksu Z. Application of biosorption for the removal of organic pollutants: A review. Process Biochemistry. 2005; 40: 997–1026.
https://doi.org/10.1016/j.procbio.2004.04.008.

14. Basar CA. Applicability of the various adsorption models of three dyes adsorption on to activated carbon prepared waste apricot. Journal of Hazardous Materials. 2006; 135: 232–241.
https://doi.org/10.1016/j.jhazmat.2005.11.055.

15. Shrivastava VC, Mall ID, Mishra IM. Characterization of mesoporous rice husk ash (RHA) and adsorption kinetics of metal ions from aqueous solutions onto RHA. Journal of Hazardous Materials. 2006; 134: 257–267.
https://doi.org/10.1016/j.jhazmat.2005.11.052.

16. McKay G, Otterburn MS, Sweeney AG. Surface mass transfer processes during colour removal from effluent using silica. Water Research. 1981; 15: 327–331.
https://doi.org/10.1016/0043-1354(81)90036-1.

17. Bereket G, Arog AZ, Özel MZ. Removal of Pb(II), Cd(II), Cu(II), and Zn(II) from Aqueous Solutions by Adsorption on Bentonite. Journal of Colloid Science. 1997; 187: 338–343. https://doi.org/10.1006/jcis.1996.4537.

18. Ho YS, McKay G. Sorption of dye from aqueous solution by peat. Chemical Engineering Journal. 1998; 70: 115–124. https://doi.org/10.1016/S0923-0467(98)00076-1.

19. Dogan M, Alkan M, Onganer Y. Adsorption of Methylene Blue from Aqueous Solution onto Perlite. Water, Air and Soil Pollution. 2000;120:229–248. https://doi.org/0.1023/A:1005297724304.

20. Mohan D, Singh KP, Singh G, Kumar K. Removal of Dyes from Wastewater Using Flyash, a Low-Cost Adsorbent. Industrial and Engineering Chemistry Research. 2002; 41: 3688–3695. https://doi.org/10.1021/ie010667+.

21. Vimonses V, Lei S, Jin B, Chow CWK, Saint C. Kinetic study and equilibrium isotherm analysis of Congo Red adsorption by clay materials. Applied Clay Science. 2009; 43: 465–472. https://doi.org/10.1016/j.cej.2008.09.009.

22. Mouni L, Belkhiri L, Bollinger, JC, Bouzaza A, Assadi A,Tirri A, Dahmoune F, Madani K, Remini H. Removal of Methylene Bluefromaqueous solutions by adsorption on Kaolin: Kinetic and equilibrium studies. Appled Clay Science. 2018; 153: 38–45. https://doi.org/10.1016/j.clay.2017.11.034.

23. Karaca S, Gurses A, Ejder M, Açıkyıldız M. Adsorptive removal of phosphate from aqueous solutions using raw and calcinated dolomite. Journal of Hazardous Materials. 2006; 128: 273–279. https://doi.org/10.1016/j.jhazmat.2005.08.003.

24. Hamed MM, Ahmed IM, Metwally SS. Adsorptive removal of methylene blue as organic pollutant by marble dust as eco-friendly sorbent. Journal of Industrial and Engineering Chemistry. 2014; 20: 2370–2377. https://doi.org/10.1016/j.jiec.2013.10.015.

25. Seyahmazegi EN, Mohammad-rezaei R, Razmi h. Multiwall carbon nanotubes decorated on calcined eggshell waste as a novel nano-sorbent: Application for anionic dye congo red removal. Chemical Enginneering Research and Design. 2016; 109: 824–834. https://doi.org/10.1016/j.cherd.2016.04.001.

26. Ozaki A, Taylor H. Kinetics and Mechanism of the Ammonia Synthesis. Proceedings of the Royal Society of London, Series A, Mathematical and Physical Sciences. 1960; 258: 47–62. https://doi.org/10.1098/rspa.1960.0174.

27. Slimani R, Ouahabi El, Abidi F, Haddad MEl, Regti A, Laamari MR, Antri SE, Lazar S. Calcined eggshells as a new biosorbent to remove basic dye from aqueous solutions: Thermodynamics, kinetics, isotherms and error analysis. Journal of the Taiwan Institute of Chemical Enggineers. 2014; 45: 1578–1587. https://doi.org/10.1016/j.jtice.2013.10.009.

28. Langmuir I. The Adsorption of gases on plane surfaces of glass, mica and platinum. Journal of the American Chemical Society. 1918; 40: 1361–1403. https://doi.org/10.1021/ja02242a004.

29. Ng C, Losso JN, Marshall WE, Rao RM. Freundlich adsorption isotherms of agricultural by-product-based powdered activated carbons in a geosmin–water system. Bioresource Technology. 2002; 85: 131–135. https://doi.org/10.1016/S0960-8524(02)00093-7.

30. Abdelwahab O. Evaluation of the use of loofa activated carbons as potential adsorbents for aqueous solutions containing dye. Desalination. 2008; 222: 357–367. https://doi.org/10.1016/j.desal.2007.01.146.

31. Dubinin MM, Radushkevich LV. Equation of the Characteristic Curve of Activated Charcoal. Proceedings of the Academy of Sciences of USSR. 1947;55:331-333.

32. Kargi F, Ozmıhcı S. Biosorption performance of powdered activated sludge for removal of different dyestuffs. Enzyme and Microbial Technology. 2004; 35: 267–271. https://doi.org/10.1016/j.enzmictec.2004.05.002.

33. Lin JX, Zhan SL, Fang MH, Qian XQ, Yang H. Adsorption of basic dye from aqueous solution onto fly ash. Journal of Environmental Management. 2008; 87: 193–200. https://doi.org/10.1016/j.jenvman.2007.01.001.

34. Dogan M, Karaoglu MH, Alkan M. Adsorption kinetics of maxilon yellow 4GL and maxilon red GRL dyes on kaolinite. Journal of Hazardous Materials. 2009; 165: 1142–1151. https://doi.org/0.1023/A:1005297724304.

35. Nadeem R, Nasir MH, Hanif MS. Pb (II) sorption by acidically modified Cicer arientinum biomass. Chemical Engineering Journal. 2009; 150: 40–48. https://doi.org/10.1016/j.cej.2008.12.001.

36. Hummers WS, Offeman RE. Preparation of Graphitic Oxide. Journal of the American Chemical Society. 1958; 80: 1339–39. https://doi.org/10.1021/ja01539a017.

37. Rafiee MA, Rafiee J, Wang Z, Song H, Yu ZZ, Koratka Nr. Enhanced Mechanical Properties of Nanocomposites at Low Graphene Content. ACS Nano. 2009; 3: 3884–3890. https://doi.org/10.1021/nn9010472.

38. Demiral H, Demiral I, Tümsek F, Karabacakoğlu B. Adsorption of chromium(VI) from aqueous solution by activated carbon derived from olive bagasse and applicability of different adsorption models. Chemical Engineering Journal. 2008; 144: 188–196. https://doi.org/10.1016/j.cej.2008.01.020.

39. Amin NK. Removal of direct blue-106 dye from aqueous solution using new activated carbons developed from pomegranate peel: Adsorption equilibrium and kinetics. Journal of Hazardous Materials. 2009; 165: 52–62. https://doi.org/10.1016/j.jhazmat.2008.09.067.

40. Han X, Wang W, Ma X. Adsorption characteristics of methylene blue onto low cost biomass material lotus leaf. Chemical Engineering Journal. 2011; 171: 1–8. https://doi.org/10.1016/j.cej.2011.02.067.

41. Menger FM, Markazi M, Mahmoodi NM, Nikkor H, Tehrani-Bagha AR. The sorption of cationic dyes onto kaolin: Kinetic, isotherm and thermodynamic studies. Desalination. 2011; 266: 247-280. https://doi.org/10.1016/j.desal.2010.08.036.

42. Acemioglu B. Batch kinetic study of sorption of methylene blue by perlite. Chemical Engineering Journal. 2005; 106: 73–81. https://doi.org/10.1016/j.cej.2004.10.005.

43. Colak F, Atar N, Olgun A. Biosorption of acidic dyes from aqueous solution by Paenibacillus macerans: Kinetic, thermodynamic and equilibrium studies. Chemical Engineering Journal. 2009; 150: 122–130. https://doi.org/10.1016/j.cej.2008.12.010

44. Haddad El, Slimani R, Mamouni R, Laamari MR, Rafqah S, Lazar S. Evaluation of potential capability of calcined bones on the biosorption removal efficiency of safranin as cationic dye from aqueous solutions. Journal of the Taiwan Institute of Chemical Enggineers. 2013; 44: 13–18. https://doi.org/10.1016/j.jtice.2012.10.003.

45. Weber WJ, Morris JC. Kinetics of adsorption on carbon from solution. Journal of the Sanitary Engineering Division. 1963; 89: 31–60.

46. Qin Q, Ma J, Liu K. Adsorption of anionic dyes on ammonium-functionalized MCM-41. Journal of Hazardous Materials. 2009; 162: 133–139. https://doi.org/10.1016/j.jhazmat.2008.05.016.

47. Alpat SK, Ozbayrak O, Alpat S, Akcay H. The adsorption kinetics and removal of cationic dye, Toluidine Blue O, from aqueous solution with Turkish zeolite. Journal of Hazardous Materials. 2008; 151: 213–220. https://doi.org/10.1016/j.jhazmat.2007.05.071.

48. Oladoja NA, Ahmad AL. Gastropod shell as a precursor for the synthesis of binary alkali-earth and transition metal oxide for Cr(VI) Abstraction from Aqua System. Separation and Purification Technology. 2013; 116: 230-239. https://doi.org/10.1016/j.seppur.2013.05.042.